Phys. Rev. 99, 376 (1955).

[34]*Footnote added in proof.* Recent calculations have yielded such quantitative information. See Weinstein *et al.* (Ref. 22 and Ref. 23.)

PHYSICAL REVIEW B VOLUME 3, NUMBER 8 15 APRIL 1971

Optical Absorption, Reflectivity, and Electrical Conductivity in GeAs and $GeAs_2$ †

John W. Rau* and C. R. Kannewurf
Department of Electrical Engineering, Northwestern University, Evanston, Illinois 60201
(Received 13 February 1970)

Single-crystal samples of two germanium arsenides were prepared: monoclinic-type GeAs and orthorhombic-type $GeAs_2$. Measurements are described for optical absorption and reflectivity in the neighborhood of the fundamental absorption edge at 300 °K and electrical resistivity over the temperature range 77–400 °K. Analysis of the optical data indicates the following: GeAs has a possible indirect band gap at 0.65 eV and direct band gaps at 1.01 and 1.65 eV; $GeAs_2$ has a possible indirect band gap at 1.06 eV and direct band gaps at 1.77 and 1.10 eV. The tailing of the absorption edge in both materials in the low-absorption region prevents a clear understanding of band structure details at the minimal band gap. Analysis of the electrical measurements for $GeAs_2$ indicates an activation energy of 0.36 eV which is associated with extrinsic behavior, carrier concentrations of the order 10^{17} cm^{-3}, and mobilities of 60 cm^2/V sec at 300 °K. All measurements are correlated with crystallographic orientation in these anisotropic materials.

I. INTRODUCTION

The use of arsenic as a doping agent to produce an *n*-type extrinsic semiconductor of germanium has been extensively studied by many workers. There are, however, two stoichiometric binary compounds GeAs and $GeAs_2$ which are known to exist and which have received very little attention in the literature. The present investigation is concerned with these two compounds.

The initial phase-diagram–composition identification of the germanium-arsenic system was proposed by Stöhr and Klemm.[1] The crystal systems were reported by Schubert *et al.*[2] to be monoclinic for GeAs and orthorhombic for $GeAs_2$. A complete structure determination was made for $GeAs_2$ by Bryden.[3] The silicon-arsenic, silicon-phosphorous, and germanium-phosphorous systems also have compounds that have the same two basic structure types.[4] From various studies of the general geometrical bonding arrangement of the atoms in the crystal structures of many compounds, Hulliger and Mooser[5] and Pearson[6] suggested that both GeAs and $GeAs_2$ should exhibit semiconducting electrical properties.

Very little is known about any of the properties of the compounds belonging to these structure types. The identification of the presence of GeAs and $GeAs_2$ in the surface layers of germanium crystals into which a large amount of arsenic, in comparison to normal extrinsic doping amounts, has been diffused was described by Waring *et al.*[7] Recent studies at this laboratory with the isotypic SiAs, primarily by optical-absorption measurements, demonstrated that the prediction for semiconducting behavior was correct for this structure type.[8] The present paper now continues this work to both optical and electrical measurements on the germanium arsenides.

II. EXPERIMENTAL

A. Sample Preparation

Ingots of both GeAs and $GeAs_2$ were prepared by the same procedure. The stoichiometric mixture of the elements[9] was heated in a sealed quartz tube that had been evacuated to a pressure of 10^{-4} Torr or less. To prevent a fracture of the quartz tube during synthesis, 14-mm-o.d. tubing with 2-mm-thick walls was employed. The temperature was increased to 750 °C over an 8-h interval, maintained at this point for 12–24 h, then slowly increased to 900 °C and held at that temperature for 3 h. The tube was then allowed to slowly cool to room temperature over a period of 12 h. The same temperature cycle was used to prepare both compounds because the melting points are nearly the same (737 °C for GeAs, 732 °C for $GeAs_2$).[1]

The introduction of one stage of zone melting as the last step in the synthesis process was found to promote the growth of larger single-crystal regions in the ingots. The ingot was cooled to just below the melting point and then passed (at a rate of 1.5 cm/h) through a narrow higher-temperature zone which was just sufficient to melt a portion of the ingot. Because the molten zone was not narrow enough to produce efficient zone refining and the

high volatility of the arsenic made it difficult to ensure that stoichiometry was not changed by this process, only one pass was made with each ingot. It was found that some GeAs ingots contained regions approximately 1 cm in diam by 2 cm long that were single crystals. Single-crystal sections of similar length, but only about 2 mm in diam, were found in $GeAs_2$ ingots.

Attempts to grow single-crystal specimens from the vapor phase with transport in vacuum or an inert gas or employing a halogen transporter were unsuccessful in producing crystals more than a few tenths of a millimeter in diameter. More elaborate techniques, such as the encapsulation method used to prepare gallium arsenide, were not employed in this initial investigation.

Both materials appear metallic gray and exhibit at least one major cleavage plane which is characteristic of most layer-structured semiconductors.

B. Crystal Orientation

1. $GeAs_2$

The crystal system as reported by Bryden[3] is orthorhombic with lattice parameters $a = 14.76$, $b = 10.16$, and $c = 3.728$ Å; space group, $Pbam$; and having 8 formula units per unit cell. Various x-ray techniques confirmed these essential features. The growth orientation of the single-crystal sample is shown in Fig. 1. The major cleavage planes are normal to the a direction. Some samples have well-defined edges along the b and c directions indicating the possible existence of secondary cleavage planes. The edge surfaces are rather irregular; this feature is not emphasized in Fig. 1. Typical sample dimensions along a, b, and c are 0.5–1 mm, approximately 2 mm, and 2–3 cm, respectively.

2. GeAs

As reviewed by Wadsten,[4] the crystal system is monoclinic with lattice parameters $a = 15.59$, $b = 3.792$, $c = 9.49$ Å, and $\beta = 101.3°$; space group, $C2/m$; and having 12 formula units per unit cell. The lattice parameters were confirmed during the identification of the growth orientation of the single-crystal material, which is shown in Fig. 1. The choice of the monoclinic unit cell shown in Fig. 1 is the same as that reported by Schubert *et al.*[2] With this choice of unit cell the cleavage plane is (001). Many samples have well-defined edges along both the a and b directions. In particular, the b direction was uniquely defined by the intersection of a secondary cleavage plane with the (001) plane. The edge surfaces are irregular. With the usual choice of the a and c directions for the monoclinic unit cell,[4] the major cleavage plane is $(20\bar{1})$. The growth orientation with respect to this unit cell has been illustrated for the isotypic SiAs.[8] The correspondence between the two unit-cell selections has been discussed by Wadsten.[10] Typical sample dimensions along the a and b directions are about 5 mm: Sample thickness varied from 0.5 to 2 mm.

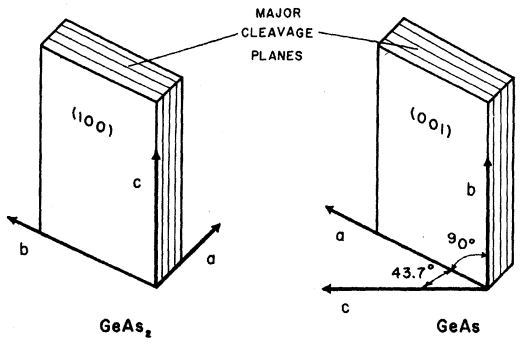

FIG. 1. Growth orientation of single-crystal samples with respect to principal crystallographic unit-cell directions (orthorhombic for $GeAs_2$, monoclinic for GeAs).

C. Reflectivity

Optical measurements were performed with a system designed for measurements of specular reflectance and absorption on samples with small surface areas. The basic system employs a Zeiss MM 12 monochromator and associated units.[11]

Reflectivity was measured by the comparison technique with the incident radiation 6° from normal incidence to the principal cleavage planes of the single-crystal samples. Over the wavelength range 0.3–2.0 μ the incident radiation was polarized along a principal crystallographic direction. For wavelengths less than 2 μ, the half-power bandwidth was less than 0.01 eV; for wavelengths longer than 2 μ, the ratio of half-power bandwidth to photon energy was less than 0.01. The results for both materials are shown in Fig. 2. These curves are the result of measurements performed on a large number of samples. All surfaces examined were from freshly cleaved material. A maximum deviation in the reflection coefficient among all samples examined of ± 0.03 from the average was observed. In some cases this was due to surface imperfections introduced by the cleaving process. No changes in reflectivity were observed for samples left exposed to laboratory atmosphere for several weeks.

D. Optical Absorption

Absorption measurements were made with polarized radiation incident normal to the principal cleavage planes of both materials over a wavelength range 0.5–5.0 μ. The resolution in terms of photon energy was 0.01 eV or better over this wavelength range. Transmission data were processed

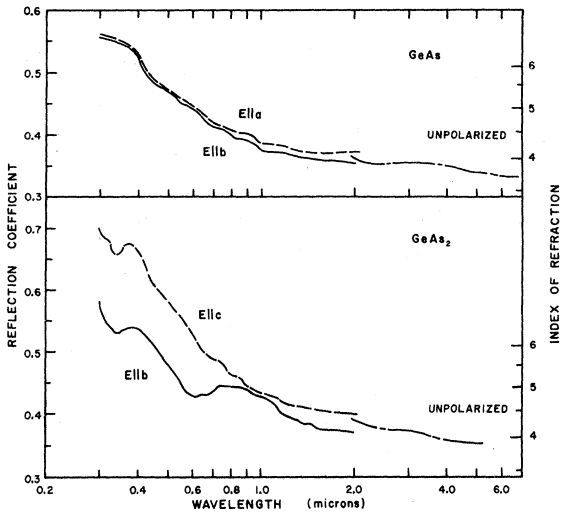

FIG. 2. Reflection coefficient at 300 °K.

by digital computer methods to obtain absorption coefficients in a manner similar to that described by Kahan.[12]

1. $GeAs_2$

In Fig. 3, the absorption coefficient for $E \| b$ and $E \| c$ is shown as a function of photon energy. These curves are the result of processing transmission data from a large number of samples with thicknesses ranging from 0.21 to 140 μ. The thinner samples were prepared by cleaving larger crystals. In the low-absorption region on the low-energy side of the fundamental absorption edge, the variation of the absorption coefficient for all samples examined was ± 15% from the typical curves shown in Fig. 3. In the high-absorption region, over the energy range 1.4–1.7 eV for the $E \| b$ curve, there is a gap in the data and an estimated section added to the curve. In this range, the over-all characteristics of the optical system combined with the high absorption in the material for that polarization and the difficulty of obtaining large-area thin samples prevented useful data from being obtained. As shown in Fig. 3, some irregularities, which are also attributed to these same factors, are present in the $E \| c$ data over this same energy range.

Some transmission data were also obtained at 77 °K in the low-absorption region up to the onset of the fundamental edge. There is only a slight shift of the absorption edge toward shorter wavelengths as the temperature decreases. At 77 °K the absorption coefficient decreases sharply in the wavelength range 3–5 μ.

2. GeAs

Figure 4 shows the absorption coefficient for $E \| a$ and $E \| b$ as a function of photon energy. Sample thickness ranged from 0.16 to 80 μ. Specimens generally had more useful surface area than those of $GeAs_2$ for approximately the same thickness. At 77 °K the absorption coefficient in the low-absorption region follows very closely the absorption curve of Fig. 4. There does appear to be a very small shift at the onset of the fundamental edge toward shorter wavelengths. The absence of any change in the profile of the curves of Fig. 4 in the low-absorption region as the temperature decreases is rather notable.

E. Electrical Conductivity

Single-crystal samples for electrical measurements were cut from ingot material with an air-borne-abrasive cutter. Ohmic contacts in the conventional four-probe arrangement were made with lead-tin solder used in conjunction with zinc-chloride flux. Measurements were performed with the samples and supporting substrate immersed in a liquid bath. Galvanomagnetic measurements were obtained with an electronic system employing as principal units a Keithley-type 610B electrometer and 147 nanovoltmeter. The output vs temperature was displayed on an x-y recorder.

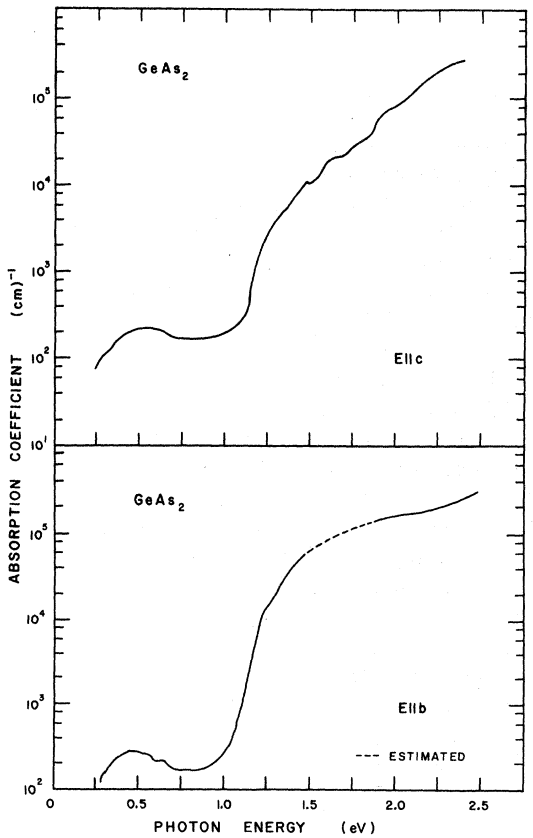

FIG. 3. Absorption coefficient vs photon energy in $GeAs_2$ at 300 °K.

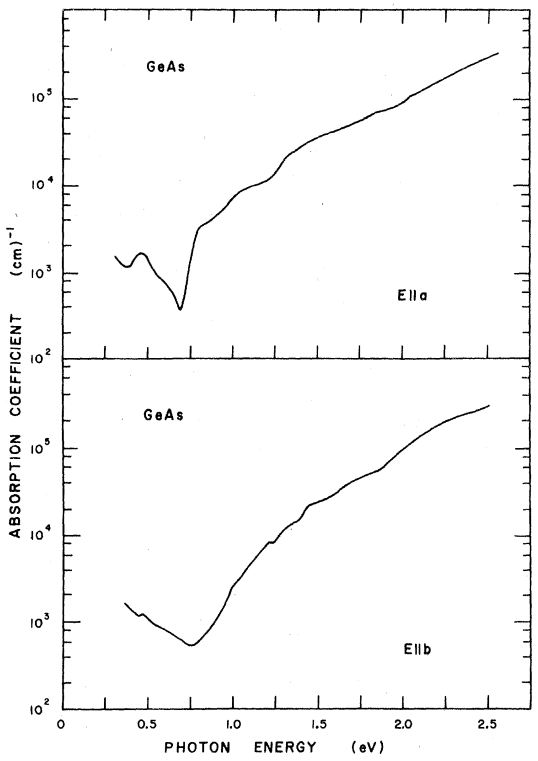

FIG. 4. Absorption coefficient vs photon energy in GeAs at 300 °K.

1. $GeAs_2$

Samples were prepared that were suitable for resistivity measurements with current I flowing along each of the principal crystallographic directions. This permits measurement of all nonzero components of the resistivity tensor for this anisotropic material. Figure 5 shows typical results from the resistivity measurements on a variety of samples. Samples 2A, 2B, and 2C were all cut from the same large single crystal and represent the highest resistivity found at low temperatures. The results for other corresponding series of three samples gave curves with the magnitude differing by less than a factor of 2 and the same slope.

Some other samples showed much lower resistivities and much less dependence of resistivity upon temperature. Samples 3 and 4 in Fig. 5 are typical of this behavior. The variation among different low-resistivity specimens appeared to be at least as great as the difference in resistivity measured with current along other crystallographic directions; thus, results are only shown for $I \| c$ in Fig. 5 to represent low-resistivity behavior.

2. GeAs

Because of the tendency of large single-crystal material to cleave very readily during mechanical operations, samples for measurements with $I \| b$ and $I \| a$ only could be prepared. Figure 5 shows the results for two samples, 11 and 12, with $I \| b$. These samples show the upper and lower limits in resistivity for all samples examined. The results for $I \| a$ did not differ significantly from those for $I \| b$: The resistivities of all samples examined also fall within the range between samples 11 and 12 in Fig. 5. Thermal probe tests indicate that all materials examined have p-type conduction.

F. Hall Effect in $GeAs_2$

Hall measurements on the high-resistivity samples were performed at 300 °K for one crystallographic orientation: $I \| c$ and the magnetic field

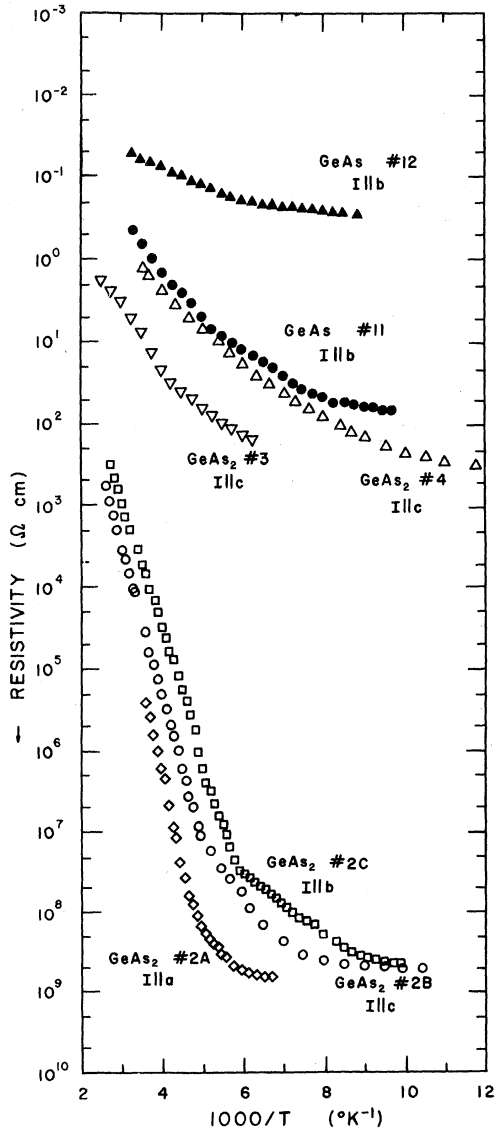

FIG. 5. Resistivity vs temperature for various samples of $GeAs_2$ and GeAs with the direction of current flow indicated for each sample.

along the a direction. All samples examined were found to be p type. The Hall voltage was found to be approximately proportional to the magnetic field strength up to fields of 12 kG. Hall data were processed using the one-carrier-model expression $R_H = 1/pe$. A summary of the electrical parameters for $GeAs_2$ at 300°K is given in Table I.

III. ANALYSIS AND DISCUSSION

1. $GeAs_2$

The absorption curves of Fig. 3 were analyzed for identification of interband-transition mechanisms. The general formulation for this analysis has been developed by Bardeen *et al.*[13] In the low-absorption region, if indirect band transitions occur, the absorption coefficient α should vary with photon energy as $(h\nu - E_g^i \pm E_p)^m/h\nu$, where m is 2 for allowed and 3 for forbidden transitions, E_g^i is the minimum energy gap, and E_p is the energy of the absorbed (+) or emitted (−) phonon participating in the transition. For direct band transitions, the absorption coefficient should vary with photon energy as $(h\nu - E_g^d)^n/h\nu$, where n is $\frac{1}{2}$ for allowed and $\frac{3}{2}$ for forbidden transitions. In a recent review, Johnson[14] has discussed the analysis of absorption data near the fundamental edge and examined the results for several III-V compounds.

In Fig. 6, a selection of data from the curves of Fig. 3 are plotted as $(\alpha h\nu)$ on a logarithmic scale vs photon energy. An attempt was made to identify on this plot the theoretical energy dependence for direct and indirect transitions. The identification of indirect band-gap transitions is somewhat hampered by the high level of background absorption ($\alpha \simeq 2\times10^2$ cm^{-1}) at the onset of the fundamental absorption edge in Fig. 3. In the $E \| c$ data, a good fit to be an allowed indirect transition energy dependence is shown which gives a band-gap value of $E_g \lesssim 1.06 \pm 0.01$ eV. In none of the indirect band transition analysis was it possible to extract any information concerning the phonon energies involved.

For the $E \| b$ data there is no strong evidence of indirect transitions. The best fit to a forbidden direct transition energy dependence over the largest energy interval in the $E \| b$ data is shown; the band-gap value is $E_g^d = 1.10 \pm 0.01$ eV. Although only the forbidden direct transition is favored in the $E \| b$ data, the possibility of an indirect transition mechanism at the threshold of the fundamental absorption edge certainly cannot be ruled out. If, in the high-absorption region of the $E \| b$ data ($\alpha h\nu > 10^4$ eV/cm), the best fit to a direct forbidden energy dependence is made, ignoring the low-absorption region, this would increase the direct band-gap value by less than 0.04 eV, which is not a significant change from the fit shown in Fig. 6.

TABLE I. Electrical parameters for $GeAs_2$ at 300°K.

	σ $(\Omega\,\mathrm{cm})^{-1}$	p (cm^{-3})	μ_p (cm^2/V sec)
$I \| a$	6.5×10^{-5}	...	...
$I \| b$	2.5×10^{-4}	5×10^{17}	60
$I \| c$	1.0×10^{-3}	...	...

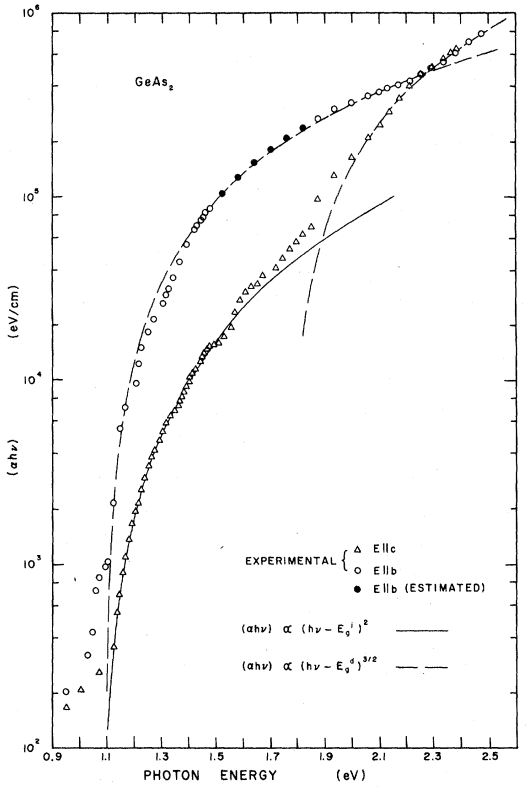

FIG. 6. $(\alpha h\nu)$ vs photon energy showing the theoretical fit to the experimental absorption edge with $E_g^i = 1.06$ eV and $E_g^d = 1.77$ eV for $E \| c$ and $E_g^d = 1.10$ eV for $E \| b$.

The entire $E \| c$ data were examined for direct transitions and only the very-high absorption region was found to suggest some evidence of a forbidden direct transition with $E_g^d = 1.77 \pm 0.03$ eV. Unlike the $E \| b$ data, the low-absorption region shows no indication of a direct transition mechanism. There is no possibility of a fit to the energy dependence for allowed direct transitions for either polarization.

From an analysis of the resistivity data for the high-resistivity samples, such as #2A, 2B, and 2C in Fig. 5, an activation energy of 0.36 eV is obtained. If this is interpreted as the result of a forbidden gap energy of $E_g = 0.72$ eV, that energy gap would be 0.34 eV lower than the smallest band gap identified in the optical data. It must be re-

membered, however, that the high-background absorption at the onset of the fundamental edge restricts the extent of the analysis in the low-absorption region and may actually mask the onset of the true minimum intrinsic gap, which might conceivably be one or two tenths of an eV less than 1.06 eV.

The rather high carrier concentration in these samples (order of 10^{17} cm^{-3}) does indicate the possibility of a sizable concentration of impurity states. All material prepared was undoped. Chemical analysis indicated the deviations from perfect stoichiometry were generally toward a deficiency in arsenic, which tends to support the thermal probe tests and Hall data indicating p-type conduction. Traces of elemental arsenic were also identified in the residue in the synthesis tubes. Thus, the activation energy might indicate the presence of some deep acceptorlike levels about 0.36 eV above the valence band. In Fig. 3, the low-absorption data of both curves do show a rather broad maximum (at approximately 0.4 eV for $E \| b$ and 0.5 eV for $E \| c$). These peaks are interpreted as evidence of some impurity absorption which may also be due to the same levels proposed from the electrical data.

Samples such as 3 and 4 in Fig. 5 are typical of the low-resistivity behavior which is much less sensitive to changes in temperature and are believed to have a much larger number of impurity levels. These levels were not identified. From spectrographic analysis, the presence of copper was detected at 0.00X%: All other impurities (Sn, Mg, Si) were less than 0.000X%. The presence of copper can be traced in part to the arsenic constituent since it was identified as present in the highest amount of all impurities in the manufacturer's spectrographic analysis of that element. In germanium and gallium arsenide, copper is known to introduce deep acceptorlike levels. But in $GeAs_2$ too few deep copper levels would be activated to account for the measured carrier concentrations.

2. GeAs

Following the same method of analysis employed for $GeAs_2$, data from the absorption curves of Fig. 4 were plotted as $(\alpha h\nu)$ on a logarithmic scale vs photon energy as shown in Fig. 7. The background absorption at the onset of the fundamental absorption is even higher than that found for $GeAs_2$. In the low-absorption region of the $E \| b$ data, a good fit is shown to the energy dependence for a forbidden indirect transition with $E_g^i \leq 0.65 \pm 0.01$ eV. There is no strong evidence of an allowed indirect transition over the same energy interval.

In the low-absorption region of the $E \| a$ data, there is no satisfactory fit to any of the recognized energy dependences for either a direct- or indirect-type transition. Rau[15] estimates the threshold energy for intrinsic absorption to be approximately 0.63 eV.

In the high-absorption region the best fit to the energy dependence for a forbidden direct transition is shown with $E_g^d = 1.01 \pm 0.01$ eV for $E \| a$ and $E_g^d = 1.65 \pm 0.02$ eV for $E \| b$. The low-absorption regions show no evidence for direct transitions. The energy dependence for allowed direct transitions does not fit the data for either polarization.

As shown in Fig. 5 for samples 11 and 12, the resistivity-vs-temperature behavior for all GeAs samples examined did not exhibit any well-defined slope from which either an extrinsic or intrinsic activation energy could be obtained. If a considerable number of different types of extrinsic levels are present in the material, then this general behavior for the electrical resistivity and low-level optical absorption might be expected.

A comparison of the curves in Fig. 4 with the corresponding optical data for the isotypic SiAs indicates a general similarity for the $E \| a$ curves. In SiAs, the $E \| b$ data also indicates a sharp rise at the onset of the absorption edge, whereas the corresponding GeAs data does not. In the high-absorption region in the neighborhood of $\alpha \sim 10^5$ cm^{-1}, the two curves of Fig. 4 cross and recross as do the curves for SiAs.[8] In the attempt to identify indirect

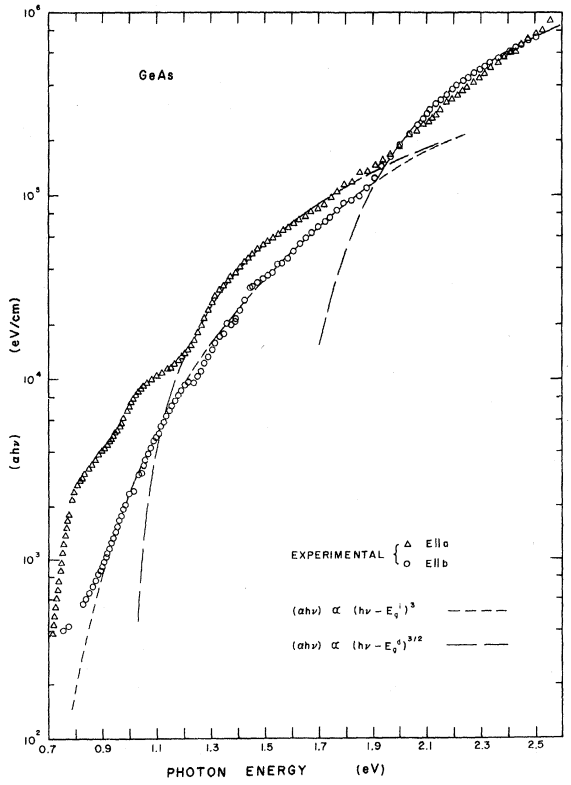

FIG. 7. $(\alpha h\nu)$ vs photon energy showing the theoretical fit to the experimental absorption edge with $E_g^i = 0.65$ eV and $E_g^d = 1.65$ eV for $E \| b$ and $E_g^d = 1.01$ eV for $E \| a$.

transition mechanisms, the same problems hamper the analysis in the low-absorption region. Direct transitions in SiAs were found over narrow energy intervals just above the proposed threshold for indirect transitions; in GeAs they occur at energies several tenths of an eV above the initial intrinsic absorption and show a better fit over a wider energy interval.

3. *General*

Of the various layer-structured semiconductors recently investigated at this laboratory, $GeAs_2$ has exhibited the most favorable transport properties and appears to be the most chemically stable under prolonged exposure to laboratory atmosphere. Many layer-structured crystals have been found to deteriorate fairly rapidly if not continually enclosed in an inert environment. Surfaces of GeAs crystals also appear quite stable in laboratory atmosphere. Spectrographic analysis of GeAs samples indicated the same results obtained for $GeAs_2$. As the initial Hall measurements on the GeAs samples were not successful, carrier mobilities are believed to be quite low.

The absorption data, for both GeAs and $GeAs_2$, do not clearly identify all band-structure details in the low-absorption region. Although there is some evidence for classifying these materials as indirect band-gap semiconductors, the tailing of the absorption edge, possibly due to impurities, may conceal some features of the minimal band gap. Such has been the case in similar studies with III-V compounds,[14] and with related compounds such as $ZnSiAs_2$.[16]

The above measurements have confirmed the preliminary identification by Hulliger and Mooser[5] and Pearson[6] of semiconducting behavior in both materials. Further work is now in progress to prepare samples with controlled extrinsic conditions for improved carrier mobilities and to better interpret the minimum intrinsic activation energy.

---

†Work based on a thesis submitted by J. W. Rau in partial fulfillment of the requirements for the Ph.D. degree. The research was supported in part by the Advanced Research Projects Agency of the Department of Defense through the Northwestern University Materials Research Center.

*Present address: The National Cash Register Company, Dayton, Ohio.

[1]H. Stöhr and W. Klemm, Z. Anorg. Allgem. Chem. 244, 205 (1940).

[2]K. Schubert, E. Dörre, and E. Günzel, Naturwiss. 41, 448 (1954).

[3]J. H. Bryden, Acta Cryst. 15, 167 (1962).

[4]T. Wadsten, Acta Chem. Scand. 21, 593 (1967).

[5]F. Hulliger and E. Mooser, J. Phys. Chem. Solids 24, 283 (1963).

[6]W. B. Pearson, Acta Cryst. 17, 1 (1964).

[7]W. Waring, D. T. Pitman, and S. R. Steele, J. Appl. Phys. 29, 1002 (1958).

[8]L. C. E. Miller and C. R. Kannewurf, J. Phys. Chem. Solids 31, 849 (1970).

[9]Germanium was obtained from the Eagle-Picher Co. in intrinsic 40-Ω-cm ingot form; arsenic from the American Smelting and Refining Co., purity: 99.999%.

[10]T. Wadsten, Acta Chem. Scand. 23, 331 (1969).

[11]J. W. Rau and C. R. Kannewurf, Zeiss Mitteilungen 5, 199 (1970).

[12]A. Kahan, Appl. Opt. 3, 314 (1964).

[13]J. Bardeen, F. J. Blatt, and L. H. Hall, in *Photoconductivity Conference*, edited by R. Breckenridge, B. Russell, and E. Hahn (Wiley, New York, 1956), p. 146.

[14]E. J. Johnson, in *Semiconductors and Semimetals*, edited by R. K. Willardson and A. C. Beer (Academic, New York, 1967), Vol. 3, p. 153.

[15]J. W. Rau, Ph.D. thesis, Northwestern University, 1970 (unpublished).

[16]G. J. Burrell, J. C. Mabberley, T. S. Moss, and J. E. Snell, Royal Aircraft Establishment, England, Technical Report No. 68115, 1968 (unpublished).